sustainability

MDPI

Article

Experimental Study on the Effect of Environmental Water on the Mechanical Properties and Deterioration Process of Underground Engineering Masonry Mortar

Jinghu Yang [1,2], Ye Cheng [1,2,*], Dawei Cui [1,2], Zewei Zhang [1,2], Bo Zhang [1,2] and Jiamei Chai [1,2]

[1] Research Institute of Emergency Science, Chinese Institute of Coal Science (CICS), Beijing 100013, China; yjh_cumtb@126.com (J.Y.); cuidawei@mail.ccri.ccteg.cn (D.C.); zhangzew16@tsinghua.org.cn (Z.Z.); zhangbo@mail.ccri.ccteg.cn (B.Z.); chaijiamei@mail.ccri.ccteg.cn (J.C.)
[2] China Coal Technology & Engineering Group (CCTEG), Beijing 100013, China
* Correspondence: chengye@mail.ccri.ccteg.cn

Abstract: Urban underground engineering is generally buried at a shallow depth and suffers long-term environmental water effects such as rainfall, rivers, underground pipeline leakage, and groundwater. The mechanical properties of the structures are affected by constant deterioration, which seriously hinders the safe, healthy, and sustainable development of the city. On the basis of on-site investigation of civil defense engineering, this article simulates the water environment conditions of mortar in underground engineering in the laboratory and conducts manual sample preparation in the laboratory. Then, water, H_2CO_3, NaCl, and Na_2CO_3 solution or wet–dry cycles are used to corrode the sample, respectively. A uniaxial compression test, Brazilian splitting test, analyses of the acoustic emission signals and electromagnetic signals, and magnetic imaging testing are performed, respectively. The results show that an increase in the action time of environmental water leads to a gradual increase in the uniaxial compressive strength, tensile strength, and elastic modulus of cement mortar, but it will decrease over a long period of time. Different environmental water components can also lead to a different performance of soaked mortar. The uniaxial compressive strength R, tensile strength σ_t, and elastic modulus E of mortar samples exhibit values in different solutions in the order of H_2CO_3 solution < NaCl solution < Na_2CO_3 solution < water. A moderate solution soak time can enhance the mechanical properties of the mortar, but this effect decreases at long time scales. The effect of wet–dry cycles on the mechanical properties and degradation process of mortar is significant. With the increase in wet–dry cycles, the porosity of mortar continuously increases. The cumulative ringing count, energy, amplitude, and impact number of acoustic emission signals always increase when the samples are loaded to failure. The uniaxial compressive strength, tensile strength, and elastic modulus first increase and then decrease. The experimental results lay the foundation for further investigating the performance changes in mortar under complex water environments in underground engineering.

Keywords: sustainable development; urban underground engineering; mechanical properties; masonry mortar; deterioration process

check for updates

Citation: Yang, J.; Cheng, Y.; Cui, D.; Zhang, Z.; Zhang, B.; Chai, J. Experimental Study on the Effect of Environmental Water on the Mechanical Properties and Deterioration Process of Underground Engineering Masonry Mortar. *Sustainability* **2024**, *16*, 5186. https://doi.org/10.3390/su16125186

Academic Editors: Andreas Angelakis and Kenneth Imo-Imo Israel Eshiet

Received: 22 April 2024
Revised: 28 May 2024
Accepted: 17 June 2024
Published: 18 June 2024

Copyright: © 2024 by the authors. Licensee MDPI, Basel, Switzerland. This article is an open access article distributed under the terms and conditions of the Creative Commons Attribution (CC BY) license (https://creativecommons.org/licenses/by/4.0/).

1. Introduction

Developing and utilizing urban underground space is one of the vital strategies to address the challenges of urban development. According to the "2022 China Urban Underground Space Development Blue Book" [1], the cumulative construction amount of urban underground space in mainland China reached 2.7 billion square meters by the end of 2021. Underground space has become an indispensable component for the sustainable and high-quality development of cities. However, issues related to disaster prevention, mitigation, and the safe maintenance of urban underground spaces have increasingly appeared. Since the construction materials of underground engineering usually use mortar

or bricks, their strength and structural stability are continuously affected by the surrounding soil and environmental water, which leads to significant safety hazards in underground spaces. For instance, there are thousands of old air raid shelters in the downtown area of Shanghai, and many of them suffer severe leakage and water accumulation; these old underground structures are highly susceptible to causing ground collapses. Therefore, it is an important study to ensure the safe and maintenance of urban underground spaces to analyze the effect of environmental water on the masonry mortar and research the safety performance of underground structures.

Currently, the research on the effects of water on mortar primarily focuses on the mixing water, such as the water content of mortar, the water-to-cement ratio, sand gradation, pH value of the water, and the effects of magnetized and electrolyzed water on the workability and strength of the mortar [2–14]. On the other hand, studies on the effects of environmental water on the mechanical properties of rocks are well-documented [15–21], which have pointed out that the action of water can reduce the strength and toughness of rocks. In terms of the impact of seawater, researchers such as Liu [22–28] have investigated the corrosion effects of sulfur-oxidizing bacteria, chloride ions, and seawater fluctuations on concrete, elucidating the patterns of change in concrete properties under seawater environments.

In the effect of environmental water on mortar performance, Giaccone D et al. [29] studied the effects of environmental water on the weight of clay bricks and lime mortar, revealing that moisture can increase the weight of masonry by over 20%. Zhou et al. [30] explored the influence of water transport and the water absorption rate on the mechanical properties of masonry walls. Bompa D V et al. [31] compared the basic mechanical properties of lime mortar masonry components in dry and humid environments. Liu et al. [32] used accelerated corrosion tests to study the erosive effects of environmental water including SO_4^{2-}, Cl^-, and Mg^{2+} on cement mortar. The results indicated that the corrosion rate is relatively slow when mortar or concrete is fully immersed in the corrosive solution. However, in alternating dry and wet conditions, there is a dual corrosion of physical and chemical factors. Liao et al. [33] studied the effects of sulfate erosion on the mechanical properties of mortar. The results showed that mortar suffered more severe damage under sulfate solution wet–dry cycles than when simply immersed in sulfate solution. The compressive strength, elastic modulus, and mass of the mortar samples showed an initial increase followed by a decrease with an increasing number of wet–dry cycles, while the peak strain corresponding to compressive strength first decreased and then increased with the increase in the number of cycles.

It can be seen that the current research on the effect of environmental water on cement mortar mainly focuses on the mixing water of cement, seawater, the wet–dry cycle effect of environmental water, and the corrosion effect of sulfate. It is evident that the research on the effect of carbonate in environmental water on mortar in underground engineering is still insufficient. Particularly, it is not clear that the effect and mechanism of environmental water on mechanical properties of mortar and deterioration process. As shown in Figure 1, this article conducts on-site investigations of early underground civil defense engineering, combined with laboratory manual sampling and geotechnical testing, to study and analyze the influence of environmental water on the mechanical properties and deterioration process of underground engineering masonry mortar under the influence of different salt solutions, action time, and wet–dry cycle numbers.

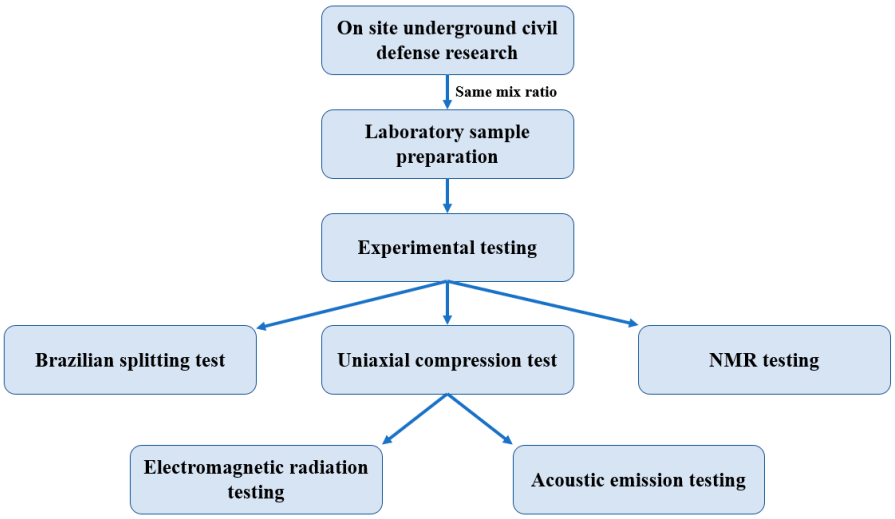
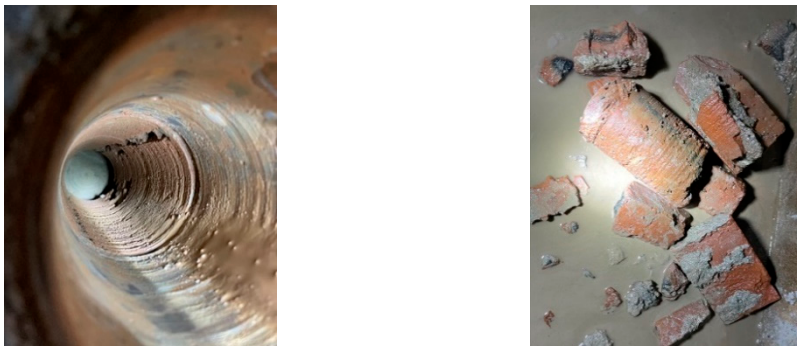


Figure 1. Research project.

2. Investigation of Water Environment for Masonry Mortar in Underground Engineering

Taking the mortar in early underground civil defense projects in Beijing as an example, the average burial depth is about −10 m, and the surrounding areas are covered with loess or sand. The internal passages of the civil defense projects composed of mortar and bricks are mostly straight wall arch structures, and multiple layers of concrete will be sprayed on the surface during later reinforcement. As shown in Figure 2, through borehole inspection, a severe void phenomenon was found between the vertical wall and the adjacent soil, which provides a channel for soil and water erosion. Additionally, the connecting of mortar and bricks have been significantly affected by the environmental water, leading to a substantial decrease in strength, which will affect the overall stability and structural safety of the civil air defense engineering.



(**a**) the void between wall and soil (**b**) Reduced mortar strength

Figure 2. Site investigation of mortar state.

According to further investigation, it can be found that the environmental water erosion of the underground civil air defense engineering primarily includes adjacent rivers, surface rainwater, a damaged subsurface supplying pipes with water, and groundwater, as shown in Figure 3. The forms of environmental water intrusion into civil air defense spaces can be classified as permeation water that filters through the soil and flowing water that enters through conduits. Permeation water is typically clear and carries soluble ions from the soil, whereas flowing water has a complex composition, is generally turbid, and may even contain biological excreta and other contaminants. The composition and properties of different environmental waters vary due to their sources. For example, Na^+, Cl^-, and CO_3^{2-} components were found in multiple underground waterproof environments.



(**a**) Sewage from the Entrance/Exit

(**b**) Pipeline leakage water

(**c**) Filtered water adjacent to river

(**d**) Crack seepage

Figure 3. Environmental water site investigation in underground air defense engineering.

Usually, groundwater is significantly influenced by seasonal variations. As shown in Figure 4, the average groundwater depth in Beijing from 2015 to 2022 was around—23 m, while in 2023, the annual average depth of groundwater was approximately—17 m, indicating an upward trend. Particularly during the rainy season, precipitation quickly percolates into the groundwater, causing a rapid rise in the water table in a short period, sometimes even higher than the depth of the civil air defense structures. Overall, the civil air defense engineering is near groundwater for extended periods, and it is also significantly eroded by groundwater.

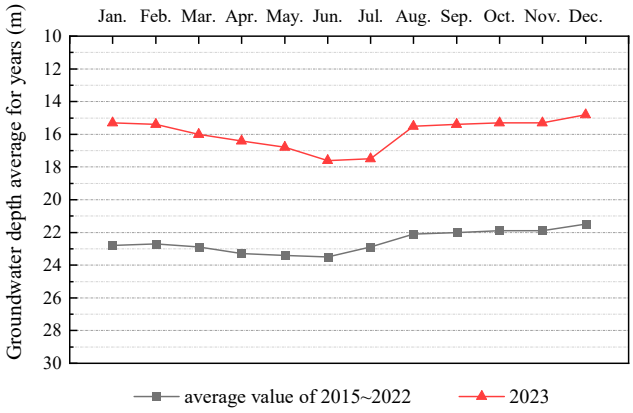


Figure 4. Groundwater depth average for many years on different months in Beijing.

3. Testing Scheme

The influence of environmental water on early underground engineering is primarily manifests as acid–base corrosion and seasonal dry and wet alternations. Therefore, this paper uses artificial mortar samples to carry out mechanical tests under different solution immersions of water, H_2CO_3, NaCl, and Na_2CO_3 under different soaking times and different dry and wet cycling conditions.

3.1. Ssample Preparation Processing

(1) Mortar sample

The mortar utilized in early subterranean civil defense structures was M7.5 masonry mortar, with a material mass ratio of "cement (325 Portland cement): quicklime (CaO): medium sand: water = 260:76:1400:324". To investigate the mechanical properties of masonry mortar for early underground civil defense structures under water environment conditions, lime mortar samples were manually prepared in the laboratory using standard molds. The samples underwent curing under standardized conditions (temperature 20 °C, humidity 95%) for 7 days and were subsequently placed in natural surroundings

(temperature 20~25 °C, humidity 30%~40%) for over 60 days. The sample set comprised 50 cylindrical specimens measuring φ50 × 100 mm and an additional set of 50 disc-shaped specimens measuring φ50 × 25 mm. Figure 5 illustrates the poured cylindrical cement mortar specimen.

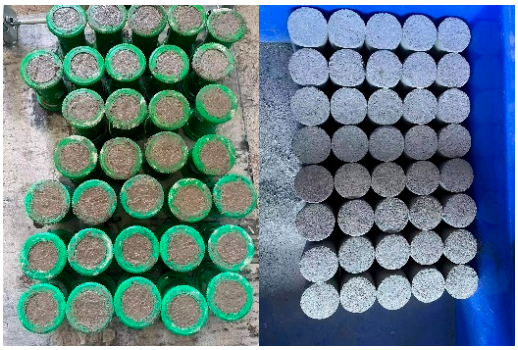


Figure 5. Samples prepared manually in the laboratory.

(2) Soaking in different solutions

Underground engineering is subject to various water environments over time, and the environmental waters typically show complex ionic compositions and show weakly acidic or weakly alkaline properties. Common ions present in these waters include Na^+, CO_3^{2-}, HCO_3^-, and Cl^-, among others. The experiment uses solutions to treat the samples by an immersion method. Different properties of environmental waters are simulated using H_2CO_3 solution, NaCl solution, and Na_2CO_3 solution. Three solutions are located in the barrels shown in Figure 6, respectively, for soaking the samples. The concentration of the three solution is 0.05 mol/L.



Figure 6. Solution used for sample immersing treatment.

As shown in Table 1, the samples are divided into 9 groups, with each group comprising 3 cylindrical samples of φ50 × 100 mm and 3 disc samples of φ50 × 25 mm.

Table 1. Sample immersing condition.

Case	Solutions	Immersion Time/d
1	H_2CO_3	10
2		20
3		30
4	NaCl	10
5		20
6		30
7	Na_2CO_3	10
8		20
9		30

(3) Wet–dry cycle of the sample

In underground engineering structures, the near-surface mortar exposed to alternating wet and dry conditions is particularly susceptible to damage. Therefore, the experiment uses an accelerated corrosion method through a wet–dry cycle. The wet–dry cycle protocol involves fully immersing the samples in water for 16 h, followed by drying in an oven at 105 °C for 8 h, which called one cycle. A total of three groups with cycle counts of 5, 10, and 20, respectively, are designated. There are 3 cylindrical samples of φ50 × 100 mm and 3 disc samples of φ50 × 25 mm in each group. After the accelerated corrosion cycles, uniaxial compressive tests, and Brazilian splitting tests are performed on these samples. Figure 7 shows the drying oven and samples during soaking.



Figure 7. Wet–dry cycle treatment.

3.2. Test Scheme

The experiments primarily applied uniaxial compressive testing and Brazilian splitting testing to evaluate the compressive strength, tensile strength, and deformation characteristics of different mortar samples. Subsequently, structural composition and microstructural features were analyzed using X-ray structural scanning and nuclear magnetic resonance (NMR) imaging.

(1) Test loading and acoustoelectric test

The pressure and acoustic emission–electromagnetic test equipment primarily consists of a loading control system, an electromagnetic shielding system, an acoustic emission-electromagnetic sensing system, and a signal acquisition system. It can conduct rock loading, unloading tests, and monitor forces, displacements, deformations, electromagnetic emissions, and acoustic emission signals. The system is shown in Figure 8.

The loading control system utilizes the YAW-600 microcomputer-controlled electro-hydraulic servo pressure testing machine. The maximum test force is 600 kN, with a load resolution of 3 N, displacement resolution of 0.3 μm. The electromagnetic shielding system employs the GP1A detachable electromagnetic shielding device, within which both the loading control system and the acoustic emission–electromagnetic sensing system are included. The acoustic emission–electromagnetic sensing system includes sensors for monitoring electromagnetic radiation and acoustic emission signals, as well as corresponding amplifiers.

In the loading process, a displacement control is used in the uniaxial compressive test and the Brazilian splitting test. The loading rate is set at 0.005 mm/s and the sampling frequency is 1 kHz. During the testing process, acoustic emission and electromagnetic signals are monitored. The electromagnetic coil is fixed at a horizontal distance of approximately 7 cm from the base of the testing machine, aligning the coil plane parallel to the loading direction, and then connected to an electromagnetic amplifier with the gain set at 64 dB. The acoustic emission sensors are secured with insulating tape around the circumference of the sample and coupled with an agent to eliminate air between the sensor and the sample surface. The sensors are then connected to an acoustic emission preamplifier with the gain set at 40 dB. The data acquisition system's sampling frequency is set at 3 MHz. Physical

parameters such as dimensions and mass of all samples are measured using vernier calipers and electronic balances, and all experiments are conducted at room temperature.

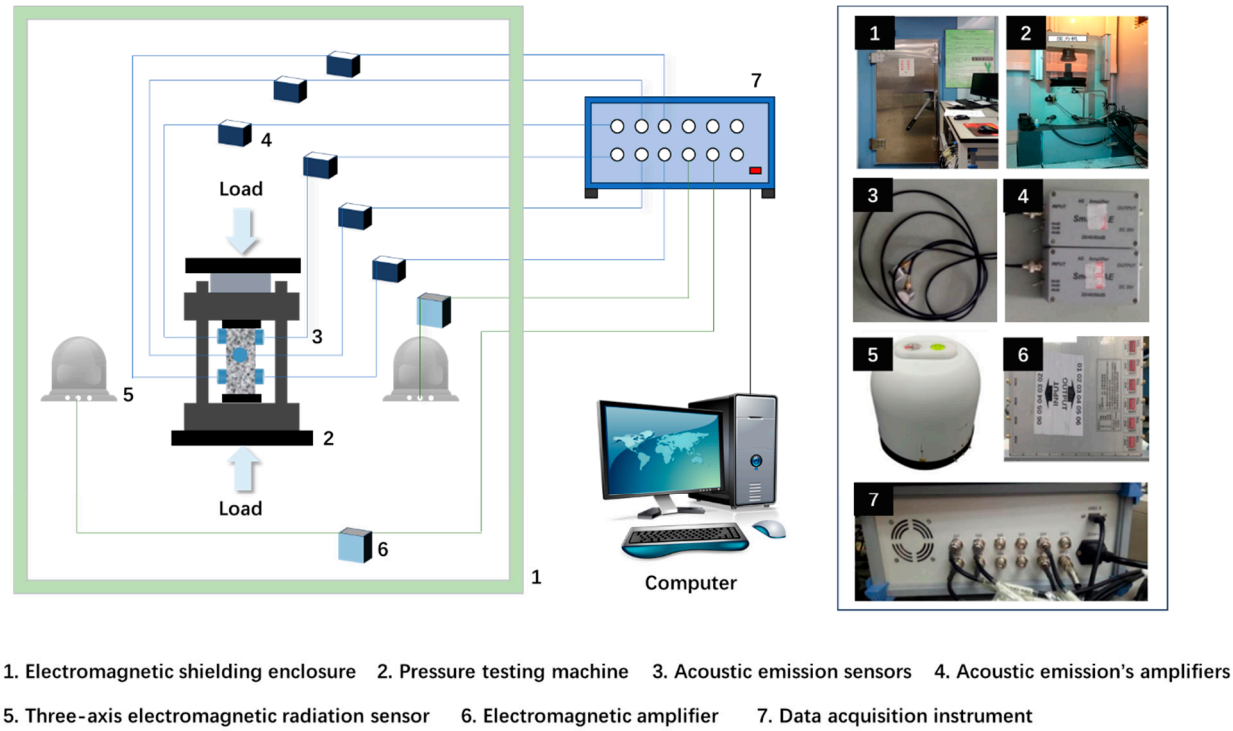


Figure 8. Pressure and acoustic emission and electromagnetic testing machine system.

The experiment follows five steps:

① Secure the acoustic emission sensors to the sample;

② Apply a preload of 200 N to the sample to ensure full contact between the press plate and the jaws;

③ Set up the loading and signal acquisition protocols, close the shielding chamber, and check the signal;

④ Start the testing machine's loading protocol and collect the signal of the load, acoustic emission, and electromagnetic radiation signals until the sample fails;

⑤ Record the experimental information, and observe the failure mode of the sample.

(2) Nuclear magnetic resonance (NMR) imaging analysis

As shown in Figure 9, the magnetic resonance imaging analyzer was produced by Suzhou Newsun, and it is used to analyze the porosity and pore size distribution of the samples.



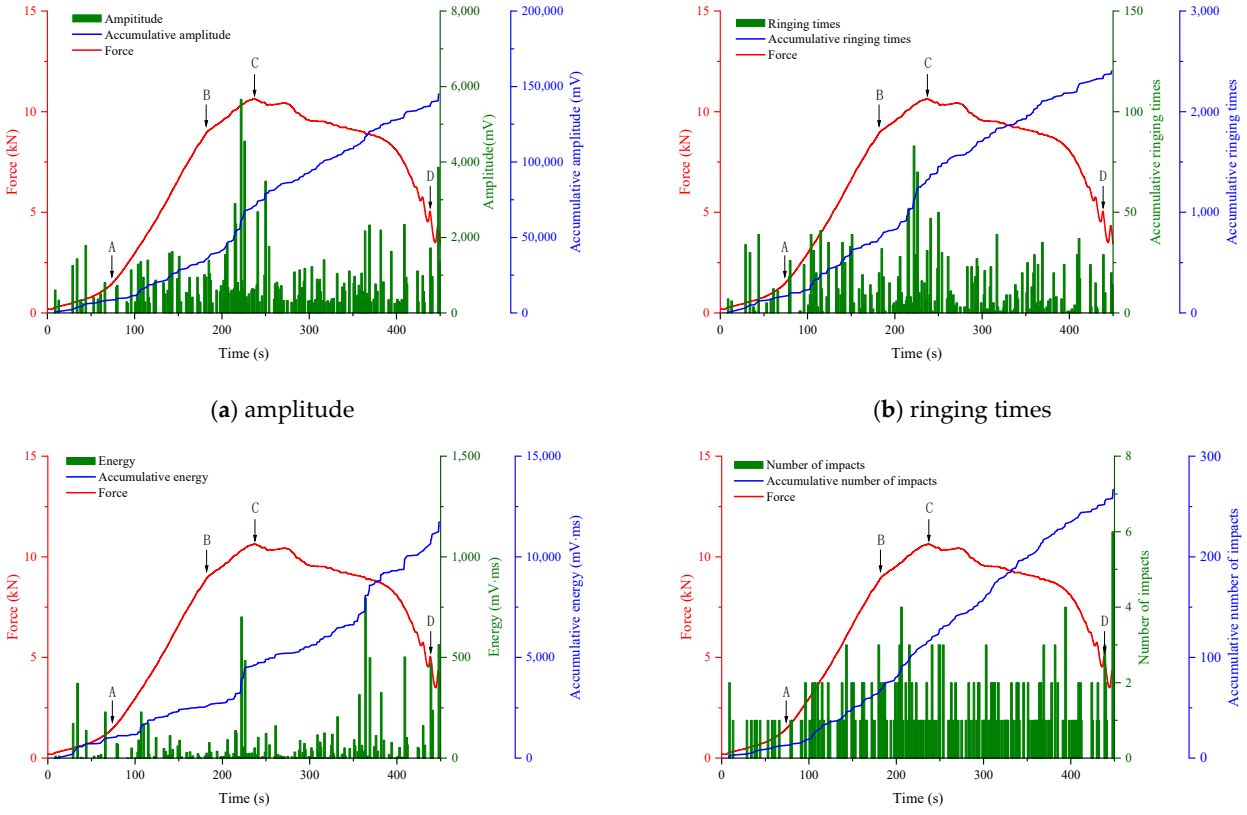
Figure 9. Magnetic resonance imaging analyzer (ME0MR23-060H-J).

The three groups' disc samples under 5, 10, and 20 accelerated corrosion cycles are immersed in water to reach a saturated state. Then, these samples are placed in the nuclear magnetic resonance imaging analysis system for porosity measurement. After the testing, the transverse relaxation time T2 spectrum curve of the pore fluid in the porous medium is obtained, and the pore structure of the samples is calculated.

4. Analysis of Testing Results

4.1. Acoustic Emission Test of Mortar Samples

According to the loading-time curve and acoustic emission parameters of the mortar samples (No. DW-2, for 5 wet–dry cycles), shown in Figure 10, the acoustic emission signals of mortar samples were analyzed through four typical stages of deformation and failure.



(**a**) amplitude (**b**) ringing times

(**c**) energy (**d**) number of impacts

Figure 10. Loading process and acoustic emission parameters changing.

(1) Stage 1, compaction stage (Section OA, 0~73.4 s)

The compaction stage of A4 is not significant. At this stage, the cracks and defects inside the sample are gradually compacted under the external load, and the mortar near the crack area is deformed and microcracked. The response of the acoustic emission signal in this stage is more significant to microdamage, especially in amplitude and energy.

(2) Stage 2, elastic deformation stage (Section AB, 73.4–181.8 s)

From a macro perspective, this stage is linearly elastic, and the load time curve is continuous. However, from a micro perspective, the deformation and fracture of the sample are discontinuous and intermittent. The acoustic emission signals show a paroxysmal characteristic as well. The acoustic emission signals are more active from 93.6 to 153.1 s, with significant responses in intensity, ringing counts, and energy.

(3) Stage 3, plastic deformation stage (Section BC, 181.8~238.0 s)

After the elastic deformation stage, some microcracks have formed inside the sample and the bearing capacity gradually decreases. At this stage, the energy has already accu-

mulated, deformation begins to accelerate, and the load increases slowly. However, the acoustic emission signal shows obvious activity during this stage, with a sudden increase in the amplitude, ringing count, and cumulative energy values.

(4) Stage 4, rupture stage (Section CD, 238.0 s~end)

At this stage, a large number of microcracks appear inside the sample, and macroscopic cracks begin to converge and connect with each other, ultimately leading to the instability and failure of the sample. From the changes in the four parameters of acoustic emission, it can be seen that the activity level of acoustic emission is significantly enhanced at this stage.

4.2. Electromagnetic Signal of Mortar Samples during the Loading and Unloading Process

During the damage of the sample under load, energy will be released in various ways, such as electromagnetic radiation. The waveform and energy diagram of the electromagnetic radiation of the mortar sample are shown in Figure 11.

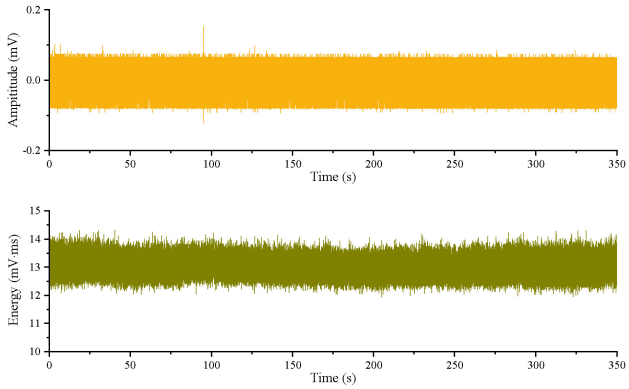
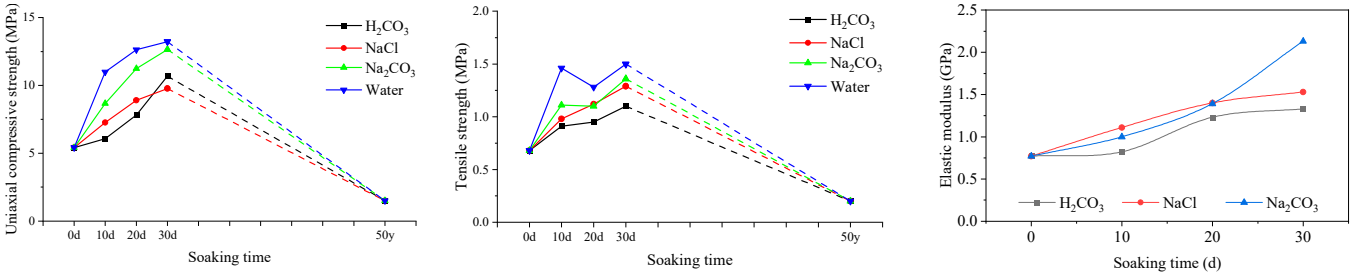


Figure 11. The waveform and energy diagram of electromagnetic radiation of mortar samples.

It can be seen that the electromagnetic signal amplitude is small in the loading process, and there is no obvious change, the signal is affected by noise seriously, and the other samples follow the same law as well. The above results indicate that the electromagnetic energy released by the mortar sample is very weak in the process of loading and destruction; hence, the damage characteristics of the mortar sample are difficult to identify through the electromagnetic signal.

4.3. Effect of Immersing Time on Mechanical Properties of Samples

Figure 12 shows the variation in mortar samples' uniaxial compressive strength, tensile strength, and elastic modulus with the increase in immersing time. And the failure energy of the sample is determined by the work conducted by the force from the beginning of loading to the maximum load, as shown in Figure 13. Figure 14 shows the variation in the compression failure energy and tensile failure energy with increasing immersing time.



(**a**) Uniaxial compressive strength (**b**) Tensile strength (**c**) Elastic modulus

Figure 12. Strength and elastic modulus under different immersing times.

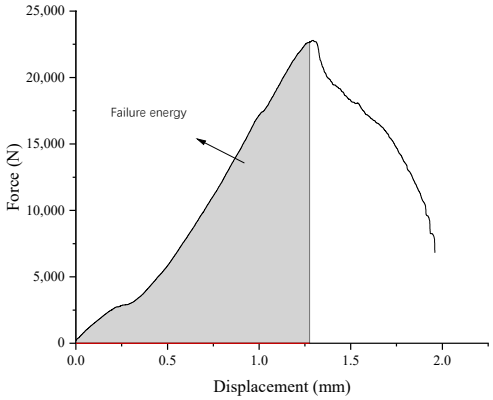
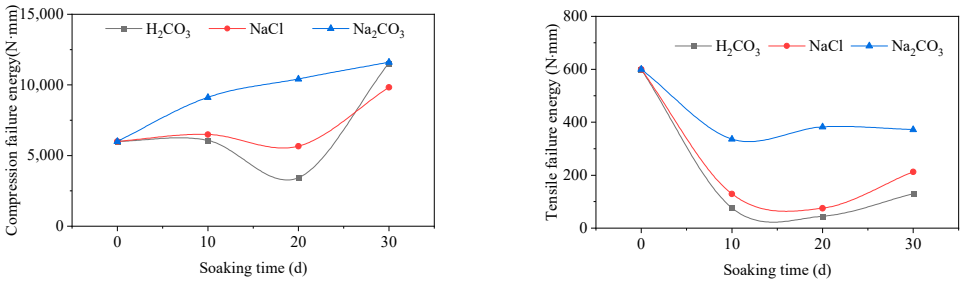


Figure 13. Failure energy.



(**a**) Compression failure energy (**b**) Tensile failure energy

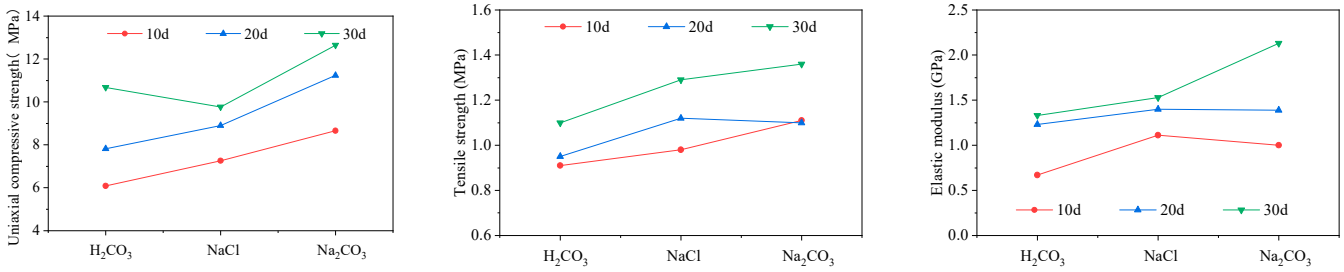
Figure 14. Failure energy under different immersing times.

It can be observed that after immersing in four solutions (H_2CO_3 solution, NaCl solution, Na_2CO_3 solution, and water), the uniaxial compressive strength R, tensile strength σ_t, elastic modulus E, and compression failure energy W_{compr} of mortar increase with the immersing time; tensile failure energy first decreases and then increases (initial strength: R = 5.42 MPa, σ_t = 0.68 MPa, E = 0.82 GPa, W_{compr} = 6000 N mm, Wtension = 600 N mm). These strength values are larger than that of the mortar drilled from the civil defense site built 50 years ago (the performance of on-site mortar is R = 1.5 MPa, σ_t = 0.2 MPa).

This is due to the fact that the mortar still contains unhydrated cement even after standard curing for 7 days and natural placement for 60 days. By immersing in different solutions, the water absorbed by mortar reacts with unhydrated cement continuously; thus, additional hydration products are produced, making the mortar more compact. With the increase in immersing time (0–30 days), the hydration reaction becomes more complete, and more hydration products appear. Macroscopically, the more the strength and modulus of elasticity of the mortar increase, the larger the destructive energy required to destroy the sample. But after a long time span (over 50 y), the hydration reaction has ended already and the cumulative effect of environmental corrosion dominates, leading to a gradual decrease in the mechanical properties of the mortar.

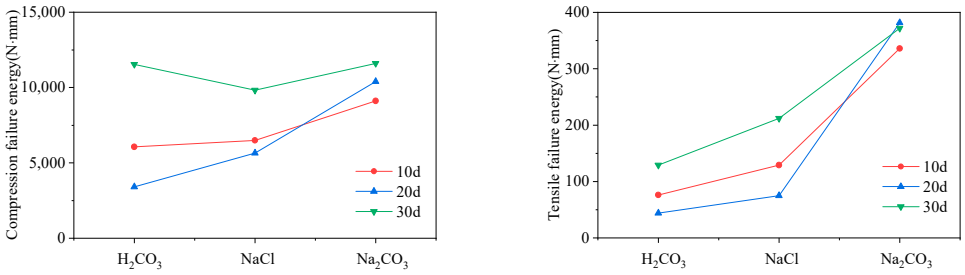
4.4. Effects of Different Solutions on the Mechanical Properties of Samples

As shown in Figures 15 and 16, the uniaxial compressive strength R, tensile strength σ_t, elastic modulus E, and failure energy W all increased after immersing in four different solutions. The values of the uniaxial compressive strength R, tensile strength σ_t, and elastic modulus E of mortar samples in these four different solutions are shown in the order of H_2CO_3 solution < NaCl solution < Na_2CO_3 solution < water.



(**a**) Uniaxial compressive strength (**b**) Tensile strength (**c**) Elastic modulus

Figure 15. Strength and elastic modulus at different solutions.



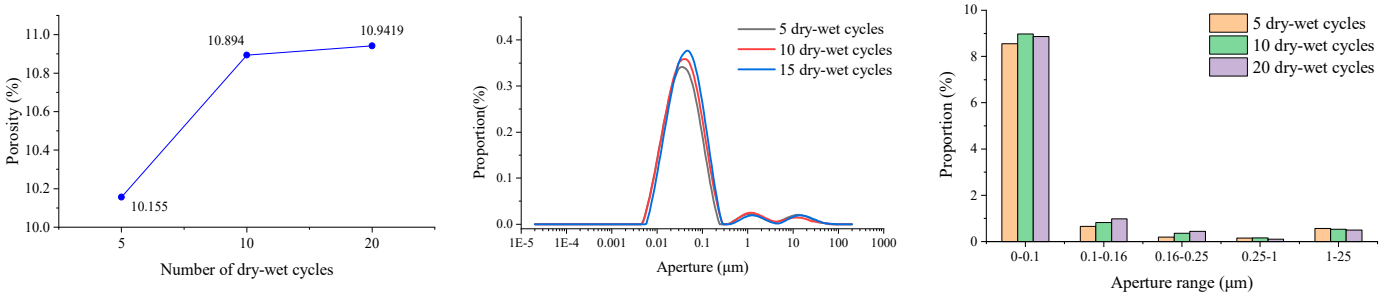
(**a**) Compression failure energy (**b**) Tensile failure energy

Figure 16. Failure energy at different solutions.

This is due to the fact that the mortar still contains unhydrated cement even after standard curing for 7 days and natural placement for 60 days. By immersing in different solutions, the water absorbed by mortar reacts with unhydrated cement continuously; thus, more hydration products are produced, making the mortar more compact. On the other hand, the reaction between H+ in H_2CO_3 and $CaCO_3$ solution leads to the chemical decomposition of $CaCO_3$, resulting in a decrease in mortar strength. The addition of NaCl increased the solubility of $CaCO_3$, resulting in the physical dissolution of $CaCO_3$ and defects in the sample, which affects the strength of the mortar.

4.5. Effects of Wet–Dry Cycles on the Mechanical Properties of Samples

Wet–dry cycles can affect the pore size distribution and porosity of mortar. As shown in Figure 17, according to the magnetic resonance imaging analysis, it can be found that the porosity of the mortar increases with the number of wet–dry cycles increases (5–20 times), although the magnitude of the increase gradually decreases. The pore size of mortar is primarily distributed in the range of 0–0.1, as shown in Figure 17c. In this interval, the percentage shows a trend of increasing and then decreasing as the number of wet–dry cycles increases.



(**a**) Variation in porosity with the wet–dry cycles (**b**) Different aperture proportions (**c**) The proportion of aperture in each interval

Figure 17. Pore size distribution and porosity.

As shown in Figure 18, through the analysis of acoustic emission signals, it can be found that the cumulative ringing count, energy, amplitude, and impact number of acoustic emission signals increase with the number of wet–dry cycles increases (0–20 times) during the loading process until failure. This is due to the fact that the wet–dry cycles increase the porosity of the mortar, and the acoustic emission signal is more active during the loading process.

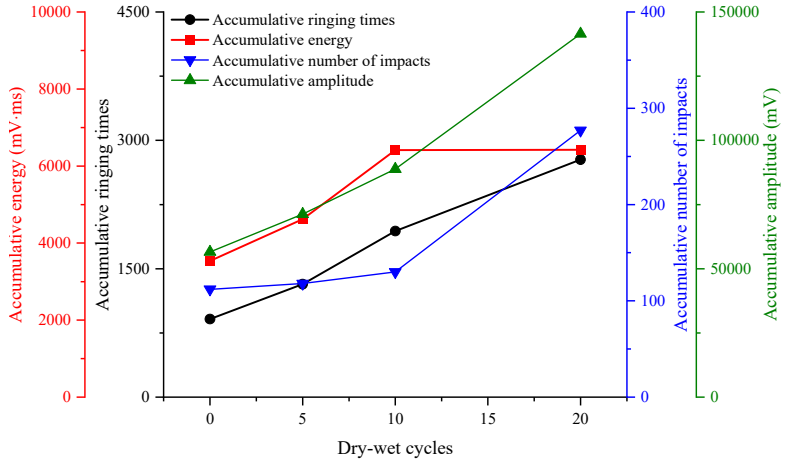


Figure 18. Variation in cumulative ring count, energy, amplitude, and number of impacts with the wet–dry cycles.

As shown in Figure 19, with the increase in wet–dry cycles, the uniaxial compressive strength R, tensile strength σ_t, and the elastic modulus E of cement mortar exhibit a pattern of first increasing and then decreasing. This is due to the fact that the mortar still contains unhydrated cement even after standard curing for 7 days and natural placement for 60 days. The first five wet–dry cycles allow the mortar to absorb moisture to react with the unhydrated cement, generating more hydration products, and the mortar become denser. The uniaxial compressive strength R, tensile strength σ_t, and elastic modulus E increase. With the persistent effect of wet–dry cycles, the stress generated by dry shrinkage and wet expansion deformation will reduce the strength of the mortar, and a stress concentration zone will be formed at the weak interface between the cement hydration products and sand, leading to the formation of micropores and microcracks. Moreover, as the number of wet–dry cycles increases, the severity of the internal damage increases and the uniaxial compressive strength R, tensile strength σ_t, and elastic modulus E subsequently decrease.

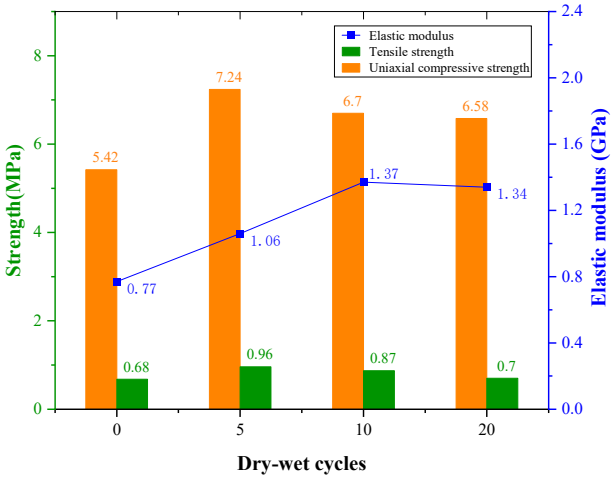


Figure 19. Compressive strength, tensile strength, and elastic modulus with the number of wet and dry cycles.

When micro-defects expand to a certain severity, there is a certain development space for dry shrinkage and wet expansion deformation. The stress generated inside the mortar will decrease; hence, the severity of further expansion of micro-defects is then reduced. Macroscopically, the rate of the mortar porosity increases and strength decrease tends to stabilize.

5. Conclusions

To study the effect of environmental water on the mechanical properties and degradation process of mortar in underground engineering, relative samples were prepared and immersed in different solution. After immersing in water, H_2CO_3 solution, NaCl solution, and Na_2CO_3 solution or via wet–dry cycles, uniaxial compression tests, Brazilian splitting tests, and acoustic emission signals, electromagnetic signals, and nuclear magnetic imaging analysis were systematically performed. The following conclusions can be drawn:

(1) Long-term exposure to rainwater, rivers, leakage from underground pipelines, groundwater, and other types of environmental water can corrode urban underground engineering structures and significantly deteriorate the mechanical properties of mortar. This poses a serious threat to the safe, healthy, and sustainable development of cities.

(2) The effect of environmental water on the mortar of underground engineering is multifaceted, among which the multi-source nature of environmental water in underground engineering generates the corrosive effect of acid–base solutions, the seasonal variation in groundwater level generates wet–dry cycle conditions, and the long service time of early underground engineering has a cumulative effect over time.

(3) The different components in environmental water can lead to different properties of mortar after immersion. Underground engineering environmental water mostly contains NaCl and Na_2CO_3 components. After immersion, the strength of mortar samples decreases compared to water immersion. The values of the uniaxial compressive strength R, tensile strength σ_t, and elastic modulus E of mortar samples in different solutions are shown in the order of H_2CO_3 solution < NaCl solution < Na_2CO_3 solution < water.

(4) The duration of exposure to environmental water has an influence on the mechanical properties of mortar. With increasing immersion time, the uniaxial compressive strength, tensile strength, elastic modulus, and compression failure energy all exhibit a gradual increase; however, eventually these mechanical properties start decreasing after a certain period of time.

(5) Wet–dry cycling conditions within underground engineering have a significant impact on both the mechanical properties and deterioration process of mortar. As the number of wet–dry cycles increases (0–20 times), the porosity of mortar correspondingly increases. The cumulative ringing count, energy amplitude, and impact number of acoustic emission signals also increase. The uniaxial compressive strength, tensile strength, and elastic modulus initially increase and then decrease.

The water environment of underground engineering is complex. Further exploration is required to study the mortar performance under a long-term scale, varying temperature, dynamic load, and other types of solutions.

Author Contributions: Conceptualization, J.Y.; methodology, J.Y. and Y.C.; project administration, J.Y.; software, B.Z.; supervision, Y.C.; visualization, J.Y. and Z.Z.; writing—original draft, J.Y. and Y.C.; writing—review and editing, D.C. and J.C.; funding acquisition, J.Y. All authors have read and agreed to the published version of the manuscript.

Funding: This research was funded by the Innovation and Entrepreneurship Science and Technology Project of China Coal Technology and Engineering Group (No. 2022-2-MS003).

Institutional Review Board Statement: Not applicable.

Informed Consent Statement: Not applicable.

Data Availability Statement: The data that support the findings of this study are available from the corresponding author upon reasonable request.

Conflicts of Interest: All authors were employed by the China Coal Technology & Engineering Group (CCTEG).

References

1. Chen, Z.L.; Jiao, D. *2022 China Urban Underground Space Development Blue Book*; Strategic Consulting Center of the Chinese Academy of Engineering: Beijing, China, 2023. (In Chinese)
2. Slapø, F.; Kvande, T.; Høiseth, K.; Hisdal, J.; Lohne, J. Mortar Water Content Impact on Masonry Strength. *Mason. Int.* **2018**, *30*, 91–98.
3. Singh, S.B.; Munjal, P.; Thammishetti, N. Role of water/cement ratio on strength development of cement mortar. *J. Build. Eng.* **2015**, *4*, 94–100. [CrossRef]
4. Dehghan, S.M.; Najafgholipour, M.A.; Baneshi, V.; Rowshanzamir, M. Experimental study on effect of water–cement ratio and sand grading on workability and mechanical properties of masonry mortars in Iran. *Iran. J. Sci. Technol. Trans. Civ. Eng.* **2019**, *43*, 21–32. [CrossRef]
5. Cuenca-Moyano, G.M.; Martin-Pascual, J.; Martin-Morales, M.; Valverde-Palacios, I.; Zamorano, M. Effects of water to cement ratio, recycled fine aggregate and air entraining/plasticizer admixture on masonry mortar properties. *Constr. Build. Mater.* **2020**, *230*, 116929. [CrossRef]
6. Wang, R.F. Experimental Study on the Performance of Permanent Magnet Magnetized Water Mortar. Doctoral Dissertation, Chang'an University, Xi'an, China, 2021. (In Chinese).
7. Xie, Z.Q.; Liu, G.B.; Zhang, T.Y.; Li, Q.Y.; Wang, L. Influence of alkaline electrolyzed water with different pH values on workability and strength of mortar. *Silic. Bull.* **2021**, *40*, 3702–3711. (In Chinese)
8. Shi, D.; Zhou, H.F.; Yang, S.F.; Xie, Z.Q.; Wang, L. Research on the influence of different types of electrolytic activated water on the hydration characteristics and strength of mortar. *Concrete* **2023**, *6*, 145–149. (In Chinese)
9. Zhou, Q.W.; Li, G.W. Experimental study on the effect of magnetized water on the performance of cement mortar. *Hydropower Stn. Des.* **2005**, *21*, 75–77. (In Chinese)
10. Zhang, T.Y.; Wang, L.; Li, Q.Y. The effect of low alkaline electrolyzed water on the performance of fly ash mortar. *Concr. Cem. Prod.* **2021**, *5*, 11–15. (In Chinese)
11. ChoiI, S.G.; Park, S.S.; Wang, K.J. Early-Age Strength of Alkali-Activated Slag Mortar Based on Burned Oyster Shell and Other Chemical Activators. *J. Mater. Civ. Eng.* **2019**, *31*, 04019186. [CrossRef]
12. Cuenca-Moyano, G.M.; Martín-Morales, M.; Valverde-Palacios, I.; Valverde-Espinosa, I.; Zamorano, M. Influence of pre-immersed recycled fine aggregate on the properties of masonry mortar. *Constr. Build. Mater.* **2014**, *70*, 71–79. [CrossRef]
13. Xie, H.; Wei, P.; Liu, N.; Gao, J.; Yang, L.; Li, J.; Chen, S. Study on failure characteristics of basalt fiber reactive powder concrete under uniaxial loading. *Constr. Build. Mater.* **2023**, *404*, 133246. [CrossRef]
14. Yang, L.; Xie, H.; Fang, S.; Huang, C.; Yang, A.; Chao, Y.J. Experimental study on mechanical properties and damage mechanism of basalt fiber reinforced concrete under uniaxial compression. *Structures* **2021**, *31*, 330–340. [CrossRef]
15. Ciantia, M.O.; Castellanza, R.D.; Prisco, C. Experimental study on the water-induced weakening of calcarenites. *Rock Mech. Rock Eng.* **2015**, *48*, 441–461. [CrossRef]
16. Wong, L.N.Y.; Maruvanchery, V.; Liu, G. Water effects on rock strength and stiffness degradation. *Acta Geotech.* **2016**, *11*, 713–737. [CrossRef]
17. Cai, X.; Zhou, Z.; Liu, K.; Du, X.; Zang, H. Water-weakening effects on the mechanical behavior of different rock types: Phenomena and mechanisms. *Appl. Sci.* **2019**, *9*, 4450. [CrossRef]
18. Chen, W.; Liu, J.; Peng, W.; Zhao, Y.; Luo, S.; Wan, W.; Wu, Q.; Wang, Y.; Li, S.; Tang, X.; et al. Aging deterioration of mechanical properties on coal-rock combinations considering hydro-chemical corrosion. *Energy* **2023**, *282*, 128770. [CrossRef]
19. Zhang, J.; Deng, H.; Taheri, A.; Ke, B.; Liu, C.; Yang, X. Degradation of physical and mechanical properties of sandstone subjected to freeze-thaw cycles and chemical erosion. *Cold Reg. Sci. Technol.* **2018**, *155*, 37–46. [CrossRef]
20. Guha Roy, D.; Singh, T.N.; Kodikara, J.; Das, R. Effect of water saturation on the fracture and mechanical properties of sedimentary rocks. *Rock Mech. Rock Eng.* **2017**, *50*, 2585–2600. [CrossRef]
21. Bian, K.; Liu, J.; Zhang, W.; Zheng, X.; Ni, S.; Liu, Z. Mechanical behavior and damage constitutive model of rock subjected to water-weakening effect and uniaxial loading. *Rock Mech. Rock Eng.* **2019**, *52*, 97–106. [CrossRef]
22. Liu, Z.H.; Gan, L.Q.; Liu, D.E.; Rong, H. The effect of sulfur oxidizing bacteria on the performance of concrete in seawater environment. *Surf. Technol.* **2023**, *52*, 280–290+317. (In Chinese)
23. Xu, F.Y.; Liang, Y.Z.; Dai, M.; Lin, L.; Liu, X.; Dai, L. A study on the effect of chloride ions in seawater on the durability of concrete. *Mod. Salt Chem. Ind.* **2022**, *49*, 56–58. (In Chinese)
24. Lv, P. A Study on the Influence of Seawater Fluctuations on the Transport Law of Chloride Ions in Concrete. Master's Thesis, Shenzhen University, Shenzhen, China, 2019. (In Chinese)
25. Han, X.Q. The Effect of the Coupling Effect of Seawater and Wet Dry Cycles on the Resistance of Concrete to Chloride Ion Penetration. Master's Thesis, Zhejiang University, Hangzhou, China, 2019. (In Chinese)
26. Jiang, W.; Sun, M.; Li, F.L. Comparison of the effects of steel fibers and PVA steel hybrid fibers on the mechanical properties of concrete under seawater corrosion. *Concr. Cem. Prod.* **2018**, *9*, 53–56. (In Chinese)

27. Liu, Y.; Jin, Z.Q.; Zhang, Y. A study on the effect of seawater on the corrosion of steel bars in concrete. *Concrete* **2016**, *6*, 38–41. (In Chinese)
28. Chen, H.Y.; Li, M.M.; Mao, J.H.; Wang, Y.; Li, Z.Y.; Yu, K.Q.; Gao, Y. The impact of seawater erosion on the early durability of concrete and maintenance measures. *Concrete* **2016**, *4*, 43–45+49. (In Chinese)
29. Giaccone, D.; Santamaria, U.; Corradi, M. An experimental study on the effect of water on historic brickwork masonry. *Heritage* **2020**, *3*, 29–46. [CrossRef]
30. Zhou, X.H.; Desmarais, G.; Vontobel, P.; Carmeliet, J.; Derome, D. Water Uptake in Masonry: Effect of Brick/Mortar Interface. In Proceedings of the 7th International Building Physics Conference, IBPC2018, Syracuse, NY, USA, 24 September 2018.
31. Bompa, D.V.; Elghazouli, A.Y. Compressive behaviour of fired-clay brick and lime mortar masonry components in dry and wet conditions. *Mater. Struct.* **2020**, *53*, 60. [CrossRef]
32. Liu, H.L.; Huang, Y.; Han, Y.P. Research on the corrosiveness of environmental water to mortar and concrete. *Concr. Cem. Prod.* **1997**, *6*, 12–15+47. (In Chinese)
33. Liao, Y.D.; Yang, Y.C.; Jiang, C.H.; Feng, X.G.; Chen, D. Degradation of mechanical properties of cementitious materials exposed to wet–dry cycles of sulphate solution. *Mater. Res. Innov.* **2015**, *19*, 173–177. [CrossRef]

Disclaimer/Publisher's Note: The statements, opinions and data contained in all publications are solely those of the individual author(s) and contributor(s) and not of MDPI and/or the editor(s). MDPI and/or the editor(s) disclaim responsibility for any injury to people or property resulting from any ideas, methods, instructions or products referred to in the content.